Journal of Ethnopharmacology 299 (2022) 115658

Contents lists available at ScienceDirect

Journal of Ethnopharmacology

journal homepage: www.elsevier.com/locate/jethpharm

Artemisia argyi extract induces apoptosis in human gemcitabine-resistant lung cancer cells via the PI3K/MAPK signaling pathway

San-Hua Su [a], Navaneethan Sundhar [b], Wei-Wen Kuo [c], Shang-Chih Lai [d,e], Chia-Hua Kuo [f], Tsung-Jung Ho [d,g,h], Pi-Yu Lin [i], Shinn-Zong Lin [j,k], Cheng Yen Shih [i], Yu-Jung Lin [b,1], Chih-Yang Huang [b,l,m,n,o,1,*]

[a] *Department of Chinese Medicine, Hualien Tzu Chi Hospital, Buddhist Tzu Chi Medical Foundation, Hualien, Taiwan*
[b] *Cardiovascular and Mitochondrial Related Disease Research Center, Hualien Tzu Chi Hospital, Buddhist Tzu Chi Medical Foundation, Hualien, Taiwan*
[c] *Department of Biological Science and Technology, China Medical University, Taichung, Taiwan*
[d] *School of Post-Baccalaureate Chinese Medicine, College of Medicine, Tzu Chi University, Hualien, Taiwan*
[e] *School of Medicine, Tzu Chi University, Buddhist Tzu Chi Medical Foundation, Hualien, Taiwan*
[f] *Department of Sports Sciences, University of Taipei, Taipei, Taiwan*
[g] *Department of Chinese Medicine, Hualien Tzu Chi Hospital, Buddhist Tzu Chi Medical Foundation, Tzu Chi University, Hualien, Taiwan*
[h] *Integration Center of Traditional Chinese and Modern Medicine, Hualien Tzu Chi Hospital, Buddhist Tzu Chi Medical Foundation, Hualien, Taiwan*
[i] *Buddhist Tzu Chi Charity Foundation, Hualien, 970, Taiwan*
[j] *Bioinnovation Center, Buddhist Tzu Chi Medical Foundation, Hualien, 970, Taiwan*
[k] *Department of Neurosurgery, Hualien Tzu Chi Hospital, Buddhist Tzu Chi Medical Foundation, Hualien, 970, Taiwan*
[l] *Graduate Institute of Biomedical Sciences, China Medical University, Taichung, Taiwan*
[m] *Department of Medical Research, China Medical University Hospital, China Medical University, Taichung, Taiwan*
[n] *Department of Biotechnology, Asia University, Taichung, Taiwan*
[o] *Center of General Education, Buddhist Tzu Chi Medical Foundation, Tzu Chi University of Science and Technology, Hualien, 970, Taiwan*

ARTICLE INFO

Keywords:
Lung cancer
Artemisia argyi
Gemcitabine resistance
Traditional Chinese medicine
Adjuvant chemotherapy

ABSTRACT

Ethnopharmacological relevance: *Artemisia argyi* H. Lév. & Vaniot (Asteraceae), also called "Chinese mugwort", is frequently used as a herbal medicine in China, Japan, Korea, and eastern parts of Russia. It is known as "ai ye" in China and "Gaiyou" in Japan. In ancient China, the buds and leaves of *A. argyi* were commonly consumed before and after Tomb-sweeping Day. It is used to treat malaria, hepatitis, cancer, inflammatory diseases, asthma, irregular menstrual cycle, sinusitis, and pathologic conditions of the kidney and liver. Although A. argyi extract (AAE) has shown anti-tumor activity against various cancers, the therapeutic effect and molecular mechanism of AAE remains to be further studied in lung cancer.

Aim of the study: This study aimed to demonstrate the anti-tumor effect of AAE and its associated biological mechanisms in CL1-0 parent and gemcitabine-resistant (CL1-0-GR) lung cancer cells.

Experimental procedure: Human lung cancer cells CL1-0 and CL1-0-GR cells were treated with AAE. Cell viability was assessed using the MTT, colony, and spheroid formation assays. Migration, invasion, and immunofluorescence staining were used to determine the extent of epithelial– mesenchymal transition (EMT). JC-1 and MitoSOX fluorescent assays were performed to investigate the effect of AAE on mitochondria. Apoptosis was detected using the TUNEL assay and flow cytometry with Annexin V staining.

Result: We found that *A. argyi* significantly decreased cell viability and induced apoptosis, accompanied by mitochondrial membrane depolarization and increased ROS levels in both parent cells (CL1-0) and gemcitabine-resistant lung cancer cells (CL1-0-GR). AAE-induced apoptosis is regulated via the PI3K/AKT and MAPK signaling pathways. It also prevents CL1-0 and CL1-0-GR cancer cell invasion, migration, EMT, colony formation, and spheroid formation. In addition, AAE acts cooperative with commercial chemotherapy drugs to enhance tumor spheroid shrinkage.

* Corresponding author. Cardiovascular and Mitochondrial Related Disease Research Center, Hualien Tzu Chi Hospital, Buddhist Tzu Chi Medical Foundation, Tzu Chi University of Science and Technology, Hualien, Taiwan.
E-mail address: cyhuang@mail.cmu.edu.tw (C.-Y. Huang).
[1] These authors contributed equally to this work.

https://doi.org/10.1016/j.jep.2022.115658
Received 12 April 2022; Received in revised form 7 August 2022; Accepted 16 August 2022
Available online 6 September 2022

Conclusion: Our study provides the first evidence that *A. argyi* treatment suppresses both parent and gemcitabine-resistant lung cancer cells by inducing ROS, mitochondrial membrane depolarization, and apoptosis, and reducing EMT. Our finding provides insights into the anti-cancer activity of A. argyi and suggests that A. argyi may serve as a chemotherapy adjuvant that potentiates the efficacy of chemotherapeutic agents.

1. Introduction

Lung cancer is among the deadliest and most common types of cancer worldwide. In 2020, 235,760 new cases of lung cancer were diagnosed, and 131,880 patients were expected to die from the disease in the USA (Siegel et al., 2020). Patients are rarely diagnosed at a localized stage (16%), which leads to a 5-year survival rate of 56%. Despite the numerous developments in treatment methods, such as surgery, radiotherapy, and chemotherapy, resistance to treatment develops rapidly.

Most chemotherapy failures are associated with the invasion and metastasis of tumors following developed chemoresistance. Upon the activation of the epithelial to mesenchymal transition (EMT) process, carcinoma cells lose their epithelial characteristics and acquire mesenchymal features (Shibue and Weinberg, 2017). Therefore, EMT activation leads to chemotherapy resistance and cancer stem cell (CSC) state activation.

Altered mitochondrial homeostasis is a prominent feature of lung cancer chemoresistance. In cancer cells, protection against programmed cell death mechanisms, such as apoptosis, represents a critical form of oncogene dependency. This increased cellular stress caused by the transformation and uncontrolled proliferation of cancer cells mainly depends on intracellular signaling pathways, including AKT/MAPK, to ensure their continued survival (Carneiro and El-Deiry, 2020). Gemcitabine (2′, 2′-difluorodeoxycytidine) is a deoxycytidine analog that is widely used to treat various solid tumors, including lung cancer (Sederholm et al., 2005). However, gemcitabine chemotherapy has been associated with cytotoxic damage to the circulatory and nervous systems, skin, and development of drug resistance (Hryciuk et al., 2018). Therefore, there is an urgent need to develop new drugs for safe, effective treatment and improved chemotherapy efficacy in lung cancer patients.

Many natural products and their derivatives are sources for most anticancer agents used in clinics for antitumor therapy, including vinblastine, paclitaxel, epipodophyllotoxins, and camptothecin (Ardalani et al., 2017; Qu et al., 2019; Venditto and Simanek, 2010; Zhu and Chen, 2019). Traditional Chinese medicine (TCM) has been practiced for millennia and is widely accepted as an alternative treatment for cancer in East Asian countries. *Artemisia argyi* H. Lév. & Vaniot (The International Compositae Alliance, TICA) is a herbaceous perennial plant that belongs to the daisy family of Asteraceae and is a widely used TCM (Song et al., 2019). Multiple East Asian countries have historical records of the use of *Artemisia argyi* for tea, food, and as a commodity (Liu et al., 2021); the whole plant has been considered a TCM for thousands of years. It is commonly used as a supplementary medicine to treat asthma, dysmenorrhea, cough, pregnancy bleeding, and allergies (Chinese Pharmacopoeia Commission, 2015; Yun et al., 2016). *Artemisia argyi* possesses multiple pharmacological activities, including immunologic, antioxidant, anti-inflammatory, and antimicrobial properties (Dhanapal et al., 2016; Hahm et al., 1998; Huang et al., 2012; Li et al., 2018; Zhang et al., 2013). One TCM practitioner has extensively used A. argyi to make herbal formulations to treat phlegm stasis breast tumors (Integrating Conventional and Chinese Medicine in Cancer Care: A Clinical Guide). In previous studies, caffeoylquinic acids, volatile oils, β-sitosterol, stigmasterol, α-amyrin, β-amyrin, friedelin, naringenin, quercetin, flavonoids, phenols, terpenoids, cylcofenchene, α-pinene, α-myrcene, D-limonene, and glycosides were isolated from *A. argyi* (Li et al., 2008; Xiao et al., 2019; Yoshikawa et al., 1996). *Artemisia* species extracts have anti-cancer properties and act by inducing apoptosis via endoplasmic reticulum-related pathways (Choi and Kim, 2013). Previous studies shown that *A. argyi* methanolic extract could activate the reactive oxygen species (ROS)-mediated apoptotic pathway to suppress colon cancer (Jeung-Min et al., 2010). It was recently reported that A. argyi essential oil inhibits hepatocellular carcinoma tumor growth and metastasis by suppressing the DEPDC1-dependent Wnt/β-catenin signaling pathway (Li et al., 2021). Moreover, phytochemicals isolated from *A. argyi* inhibit metastasis and angiogenesis in several cancer types (Lee et al., 2005; Tseng et al., 2020; Zhang et al., 2018). However, there are few formal scientific inquiries to supporting the anti-cancer property of this herbal medicine, and its molecular targets in lung cancer remain unknown.

Here, for the first time we report the anti-cancer activity of A, argyi in lung cancer CL1-0 parent and CL1-0-GR cells. *Artemisia argyi* extract showed inhibition of cell proliferation, cell aggregation, EMT, and metastasis in CL1-0 parent and CL1-0-GR cells. Furthermore, AAE induced mitochondrial membrane depolarization, and apoptosis and inhibited AKT/MAPK signaling in two lung cancer cell lines, supporting its potential value as an adjuvant treatment that increases the efficacy of established chemotherapeutic agents.

2. Materials and methods

2.1. Extract preparation

Artemisia argyi Lévl et Vant was identified and verified by Dr. Tamilselvi Shanmugam and deposited at the herbarium in the Department of Chinese Medicine, Tzu Chi University. No 03. (Hualien, Taiwan). The aerial parts (leaves) of *A. argyi* were washed in fast-flowing tap water to eliminate surface dirt. The plant material was dried, cut, and then ground to powder using a mechanical blender. Dried powdered leaves of *A. argyi* (10 g) were extracted with 500 mL of distilled water. Subsequently, the homogenate was filtered using a 0.4-μm filter and final concentrated was obtained 50 mg/ml. The obtained AAE was stored at 4 °C prior to use. The extraction method was performed as previously described, with minor modifications (Wu et al., 2020).

2.2. Chemicals and reagents

In this study, 2′,2′-difluorodeoxycytidine (gemcitabine) was purchased from Eli Lilly Company (Indianapolis, IN, USA). Doxorubicin (catalog number: D1515), oxaliplatin (catalog number: 09512), irinotecan (catalog number: I1406), paclitaxel (catalog number: T7402), 3-(4,5-dime-thylthiazol-2-yl)-2,5-diphenyltetra-zolium bromide (MTT), and 5,5′,6,6′-tetrachloro-1,1′,3,3′-tetraethylbenzimidazolocarbocyanine iodide (JC-1) assay kits were purchased from Sigma-Aldrich (St. Louis, MO, USA). MitoSOX Red was purchased from Molecular Probes (Invitrogen, Carlsbad, CA, USA). The following primary antibodies were used: E-cadherin, caspase-3, Bak, Bcl-2, β-actin, AKT, p-AKT, p-ERK1/2, SOD-1, Catalase (Santa Cruz, CA, USA), cleaved Caspase-3, vimentin (Cell Signaling Technology, Danvers, MA, USA), AKT, and Bcl-2 (BD Biosciences, San Jose, CA, USA). The anti-rabbit immunoglobulin G (IgG) and anti-mouse IgG HRP-conjugated secondary antibodies were purchased from Santa Cruz Biotechnology (Santa Cruz, CA, USA).

2.3. Cell lines and cell culture

The lung adenocarcinoma cell line CL1-0 was kindly provided by Prof. Pan-Chyr Yang (National Taiwan University College of Medicine) (Chu et al., 1997). Drug-resistant CL1 cell line was established by

exposing a CL1 cell line to doses of 0–40 μM gemcitabine. The surviving cells were recovered to 75% in a culture plate and then passaged in the same gemcitabine concentration to increase the gemcitabine dose until 40 μM. Both cell lines were maintained in RPMI medium supplemented with 10% fetal bovine serum (FBS), 100 U/ml penicillin, and 100 μg/ml streptomycin at 37 °C in a 5% CO2 humidified atmosphere. The cells were cultured in RPMI-1640 medium (Gibco, Grand Island, NY, USA) supplemented with 10% FBS (Gibco) at 37 °C in a humidified atmosphere with 5% CO2.

2.4. Wound healing assay

CL1-0 and CL1-0-GR cells were seeded in 12-well plates (1.5×10^5 cells) and grown to 70–80% confluence. Straight scratches were made using 200 μL sterile pipette tips and washed by PBS to remove cell debris. Cells were then cultured with serum free media containing. Cell migration into the wound area was photographed at 0 and 24 h using an inverted microscope and quantified using Image J.

2.5. Transwell invasion assay

In vitro cell invasion assay was performed using a chamber coated with Matrigel (200 μL) and transwell chambers (8 μm pore size; SPLInsert™ hanging 24-well plate). Cells (4×10^4) were plated in serum-free media in the upper chamber. Media with 10% FBS in the lower section served as a chemoattractant. After 48 h, non-invading cells were removed from the upper chamber using cotton swabs, and the invasive cells on the lower chamber were stained with crystal violet, air-dried, photographed, and counted. The invading cells were counted using 20 × magnification under a Zeiss microscope (Axio Vert A1, Oberkochen, Germany).

2.6. Immunofluorescence staining

CL1-0 and CL1-0-GR cells (15×10^3 per 200 μl) were treated with 500 μg AAE for 48h and fixed for 45 min with 4% paraformaldehyde at room temperature (RT), then washed three times with PBS. The samples were incubated overnight at 4 °C with either anti-E-cadherin antibody (1:100 dilution; Cell Signaling) or anti-vimentin antibody (1:250 dilution; Santa Cruz) in PBS. The samples were subsequently rinsed with PBS three times and incubated for 1 h at RT with the appropriate dye-conjugated Alexa Fluor® 594 and Alexa Fluor® 488 secondary antibodies (1:100 dilution; Thermo Fisher). Finally, the samples were rewashed with PBS and sealed with a mounting medium containing 4′,6-diamidino-2-phenylindole (DAPI) (Abcam). All images were observed using an Axio Observer A1 digital fluorescence microscope (Olympus, Tokyo, Japan).

2.7. Spheroid formation

A total of 10,000 CL1-0 parent or CL1-0-GR cells were seeded in 100 μL of a complete media at the indicated concentrations of AAE in 96-well microtiter μ-bottom plates. CL1-0 and CL1-0 gemcitabine-resistant (CL1-0-Gem-R) cells were incubated for 7–10 days at 37 °C and 5% CO2 until spheroids formed. The aggregated cancer cell area and density were estimated using the ImageJ software; ReViSP was used to determine the associated 3D structures.

2.8. JC-1 staining

JC-1 dye has been established to detect ΔΨm in healthy and apoptotic cells. The growth medium was aspirated from the flask, and the cells were overlaid by the JC1- staining solution (Sigma Aldrich, Catalog number CS0390). For 1 cm^2 of growth surface, add 0.2–0.4 ml of the Staining Mixture. Cells were incubated in a humidified atmosphere containing 5% CO2 at 37 °C for 15–20 min. Cells were rinsed twice with a growth medium. Finally, images were captured in the green and red fluorescence channel in the inverted fluorescence microscope (Olympus, Tokyo, Japan). The images were obtained at 490 nm excitation and 530 nm emission for green (JC-1 monomers) and at 525 nm excitation and 590 nm emission for red fluorescence (JC-1 aggregates).

2.9. Determination of ROS production

MitoSOX Red fluorescent probe was used to determine the mitochondrial generated ROS. MitoSOX Red reagent, a live-cell permeant, selectively targets mitochondria and exhibits red fluorescence when oxidized by superoxide. Cells were incubated for 30 min in 2.5 μM MitoSOX Red in PBS. Then, the cells were imaged using a fluorescence microscope (Olympus, Tokyo, Japan).

2.10. Terminal deoxynucleotidyl transferase dUTP nick end labelling (TUNEL) assay

CL1-0 and CL1-0-GR cells (15×10^3 per 200 μl) were treated with 300 and 500 μg AAE for 36 h, washed with 1 × PBS and incubated in a fixation solution (4% paraformaldehyde in 1 × PBS at pH 7.4) at RT for 1 h. Permeabilizing solution (0.1% Triton X–100 in 0.1% sodium citrate) was added to the cells, and the plate was placed on ice for 2 min. Subsequently, the cells were stained using a transferase dUTP nick end labelling (TUNEL) reagent (Enzyme Solution and Label Solution [*In Situ* Cell Death Detection Kit], Roche, Indianapolis, IN) and incubated at 37 °C in the dark for 1 h. Finally, the cells were washed using PBS and overlaid with DAPI. Fluorescence was assessed using a digital fluorescence microscope (Olympus, Tokyo, Japan).

2.11. Determination of apoptosis by annexin V and propidium iodide staining

The induction of apoptosis in CL1-0 and CL1-0-GR cells by AAE was analyzed using a fluorescein isothiocyanate (FITC) Annexin V Apoptosis Detection Kit I (BD Biosciences, Franklin Lakes, NJ, USA) according to the manufacturer's protocol. Briefly, 5×10^5 cells were seeded in a six-well plate and treated with different AAE concentrations for 36 h at 37 °C. Adherent cells were detached with trypsin-EDTA. The cells were centrifuged, washed twice with PBS, and resuspended in 1 × binding buffer. Then, 100 μL of the cell suspension was transferred to a 5 mL culture tube and incubated with 5 μL FITC Annexin V and 5 μL propidium iodide (PI) for 30 min at RT in the dark. Finally, 400 μL of 1 × binding buffer was added to a 5 mL culture tube. Fluorescence intensity was analyzed using flow cytometry.

2.12. Colony formation assay

In this study, CL1-0 and CL1-0-GR cells were seeded in six-well plates at a density of 500 cells/well and cultured with various concentrations of AAE. After 14 days, the cells were washed three times with PBS, fixed with 4% paraformaldehyde for 30 min, and stained with Giemsa for 15–30 min. Subsequently, the number of colonies was counted (Kannathasan et al., 2020).

2.13. Quantitative real-time polymerase chain reaction analysis

All primers listed in Table 1 were synthesized by PROTECH (Taipei, Taiwan). The cDNA was synthesized using a Revert Aid First Strand cDNA Synthesis Kit (Thermo) to detect mRNA of CL1-0 and CL1-0-GR cells treated with 500 μg AAE for 48h. Quantitative real-time polymerase chain reaction (qRT-PCR) was accomplished using SYBR Green PCR Master Mix (Bio-Rad). We used a QuantStudio 5 RT-PCR System following the manufacturer's guidelines, using a total reaction volume of 20 μL that contained 10 μL SYBR Green PCR Master Mix, 1 μl of forward and reverse primers, and 100 ng of cDNA. The reaction mixtures

Table 1
Primer sequence for qRT-PCR.

Gene symbol	Forward primer	Reverse primer
E-cadherin	*GAGCCTGAGTCCTGCAGTCC*	*TGTATTGCTGCTTGGCCTCA*
Vimentin	*TCCAGCAGCTTCCTGTAGGT*	*CCCTCACCTGTGAAGTGGAT*
TJP-1	*ACCAGTAAGTCGTCCTGATCC*	*TCGGCCAAATCTTCTCACTCC*
ABCC10	*CGGGTTAAGCTTGTGACAGAGC*	*AACACCTTGGTGGCAGTGAGCT*
CYP3A5	*GGTGGTGATTCCAACTTATGC*	*GCGTGTCTAATTTCAAGGGGA*
GAPDH	*GCACCGTCAAGGCTGAGAAC*	*TGGTGAAGACGCCAGTGGA*

were incubated in an Applied Biosystems qRT-PCR 96-well tube at 95 °C for 3 min, followed by 40 cycles at 95 °C for 15 s, 55 °C for 30 s, and 72 °C for 30 s. All reactions were performed in triplicate. The cycle number at which the response to cross the threshold cycle was determined for each gene.

2.14. Western blotting

Using standard procedures western blot analysis was performed (Hsu et al., 2019). Cells from both cell lines were treated with 300 & 500 μg AAE for 48h and lysed with radioimmunoprecipitation assay buffer. Next, 30 μg of protein was resuspended in a loading buffer, separated by 8% SDS-PAGE gel, and electrophoretically transferred to a nitrocellulose membrane. The membrane was blocked with 5% bovine serum albumin for 1 h, followed by overnight incubation with the primary antibodies. Next, the membrane was washed three times for 10 min with PBST and incubated with a horseradish peroxidase-linked secondary antibody (1:5000) for 1 h in blocking solution. Later the membrane was washed three times with PBST for 10 min, and bands were visualized using an automatic fluorescent cold light biomedical imaging system (UVP Che studio plus).

2.15. Statistical analysis

All statistical analyses were performed using GraphPad Prism v5.0.3.477 (GraphPad Software Inc., San Diego, CA). The data are expressed as mean ± standard error. Based on their normality of distribution (Shapiro-Wilk test) data were analyzed by one-way analysis of variance (ANOVA). Student's *t*-test was performed to compare of the means between two groups. All results were quantified using ImageJ software (NIH, Bethesda, MD, USA). *p < 0.05, **p < 0.01 and ***p <

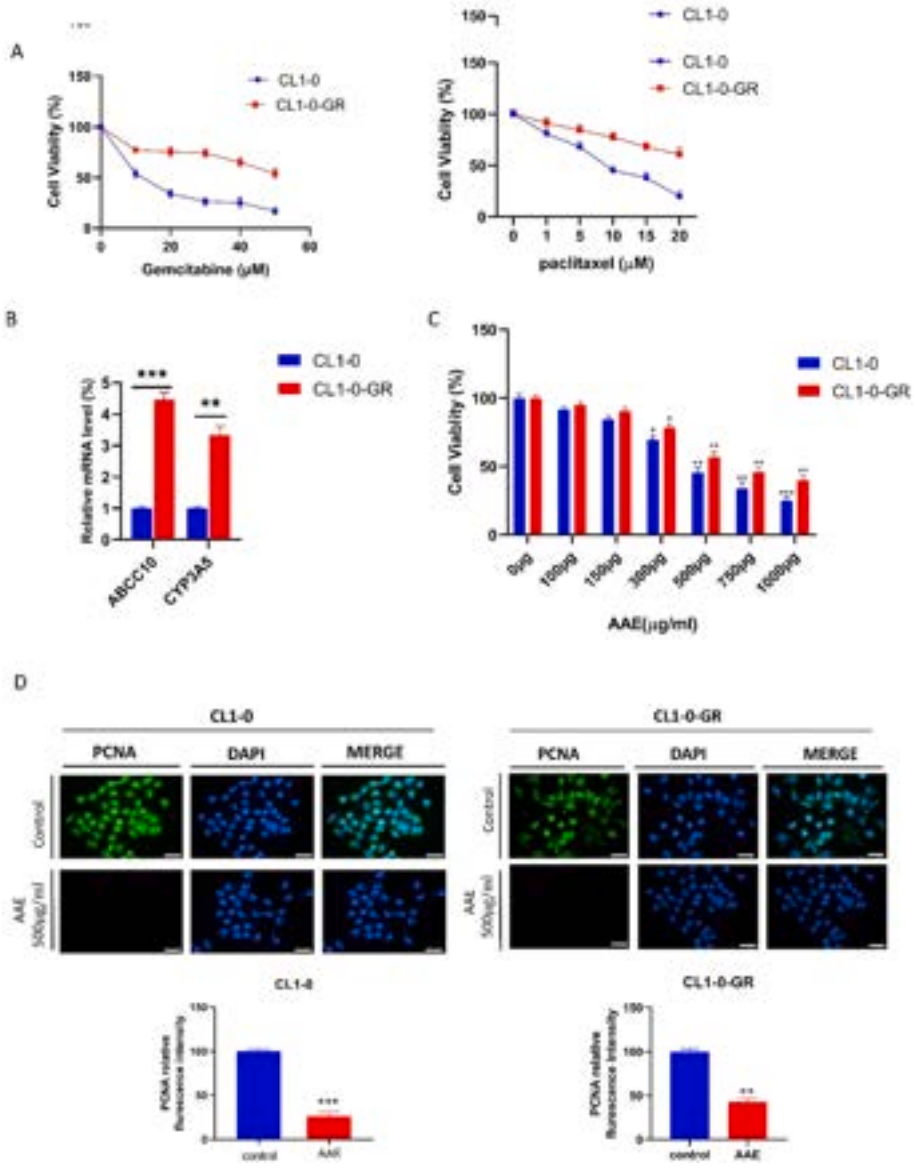

Fig. 1. Effect of *Artemisia argyi* water extract (AAE) on CL1-0 parent and gemcitabine-resistant (CL1-0-GR) lung cancer cell proliferation. (A) Gemcitabine- and paclitaxel-induced chemoresistance in CL1-0 lung cancer cell lines. CL1-0 and CL1-0-GR cells were treated with gemcitabine [0–50 μM] and paclitaxel [0–25 μM] for 48 h, and cell viability was assessed using the MTT assay. Cell viability decreased in a dose-dependent manner in CL1-0 but not in CL1-0-GR cells. (B) Quantitative polymerase chain reaction analysis of ABCC10 and CYP3A5 levels in CL1-0 and CL1-0-GR cells after treatment with AAE (500 μg) for 48 h. (C) The CL1-0 and CL-1-0-GR cells were treated with different concentrations of AAE (up to 1000 μg). The 3-(4, 5-dimethylthiazol-2-yl)−2,5-diphenyltetrazolium bromide assay was used to measure cell viability. (D) Immuno-reactive proliferating cell nuclear antigen (PCNA) was analyzed in response to AAE treatment for 48 h. PCNA expression was high in non-treated CL1-0 and CL1-0-GR cells and low in both sets of AAE-treated cells. Cells were counterstained with DAPI (blue) for nuclei. Green fluorescence intensity was quantified using ImageJ. Scale bar, 100 μm. Data are shown as the mean ± standard error of values obtained in at least three independent experiments, ***p < 0.001, **p < 0.01, *p < 0.05 compared with control cells. (For interpretation of the references to color in this figure legend, the reader is referred to the Web version of this article.)

0.001 were considered statistically significant.

3. Results

3.1. Chemoresistance and AAE effects on lung cancer cells

The MTT assay was used to evaluate the level of drug resistance of CL1-0-GR cells at varying concentrations of two kinds of chemotherapeutics (gemcitabine [0–50 μM] and paclitaxel [0–25 μM]). Cell viability decreased in CL1-0 cells in a dose-dependent manner. However, CL1-0-GR cells showed no significant reduction in cell viability due to gemcitabine or paclitaxel (Fig. 1A). It has been reported that ABCC10 and CYP3A5 are the predictive molecular marker for gemcitabine-resistant lung cancer (Ikeda et al., 2011). Consistent with this study, the expression of ABCC10 and CYP3A5 was higher in gemcitabine-resistant CL1-0 cells compared to parent cells (Fig. 1B). Next, we investigated the effect of AAE on parental (CL1-0) and chemo-resistant (CL1-0-GR) lung cancer cells. Cells were treated with increasing concentrations of AAE (100, 150, 300, 500, 750, and 1000 μg) for 48 h, and cytotoxicity was assessed using the MTT assay. Compared to the control group, the AAE-treated cells presented decreased cell viability in a dose-dependent manner (Fig. 1C). Cell viability was decreased by 50% at 500 μg of AAE in both CL1-0 and CL1-0-GR cells. Based on these results, 500 μg of AAE was used in future experiments to determine its other anti-cancer effects. In addition, we used immunostaining to determine the expression of the proliferation marker PCNA in CL1-0 and CL1-0-GR cells. After treatment with AAE, the fluorescence intensity was reduced in both CL1-0 and CL1-0-GR cells (Fig. 1D). These findings suggest that AAE can inhibit lung cancer cell proliferation.

3.2. AAE inhibits migration, invasion, and EMT in parent and gemcitabine-resistant CL1-0 cells

EMT is an initial step for cancer cells to obtain invasive properties. Scratch and Matrigel-coated transwell assays were used to test the migration and invasion abilities of the CL1-0 parent and CL1-0-GR cells after treatment with AAE. AAE inhibited the migration and invasion of parent and gemcitabine-resistant cells in a dose-dependent manner when compared to the control group (Fig. 2A and B). CL1-0 and CL1-0-GR cells were treated with 500 μg of AAE for 48 h. Afterward, E-cadherin and vimentin, which are EMT markers, were stained to observe the fluorescence intensity. AAE increased the expression levels of E-cadherin and decreased the vimentin expression (Fig. 2C). Next, we investigated the mRNA expression of EMT-related genes, E-cadherin, vimentin, and TJP-1. The mRNA expression of vimentin and TJP-1 significantly decreased following treatment with 500 μg of AAE in CL1-0 and CL1-0-GR cells. Levels of a critical component of the adherent junction, E-cadherin, increased following AAE treatment (Fig. 2D). These results indicate that AAE suppresses the migration, invasion, and EMT of lung cancer cells.

3.3. Restriction of colony and spheroid formation by AAE in CL1-0 and CL1-0-GR cells

We next examined AAE's effect on the clonogenicity of both CL1-

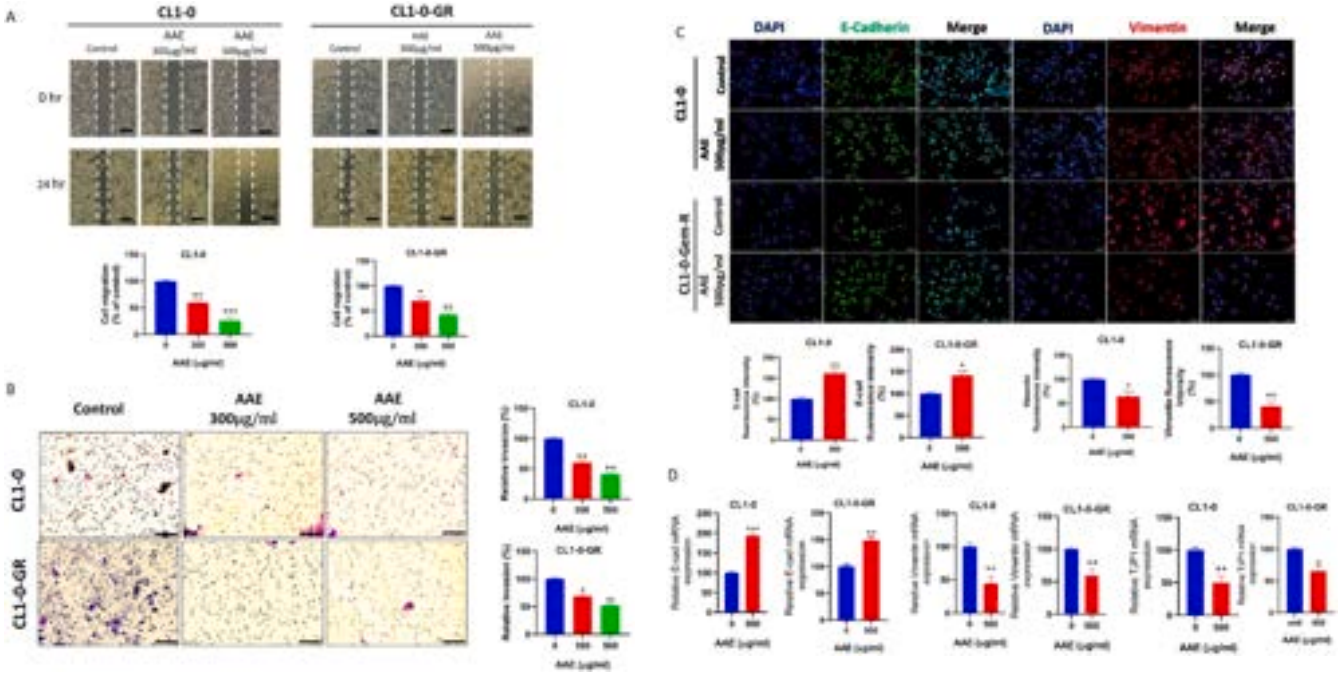

Fig. 2. ***Artemisia argyi*** **water extract (AAE) suppresses the migration, invasion, and EMT of lung cancer cells**. Wound healing assay and transwell invasion assays of CL1-0 and CL1-0-GR cells were treated with the indicated concentration of AAE. (A) Cell migration was detected by wound healing assay. Images were captured at 0 and 24 h incubation with AAE (300 and 500 μg/mL) and migration percentage was measured. Scale bar, 50 μm (B) The invading cells were visualized by crystal violet staining and observed with a light microscope (magnification, 100 ×). ImageJ was used to quantify the cell migration rate. Scale bar, 100 μm. Data are presented as the mean ± standard deviation (SD) from three observed fields. ***p < 0.001, **p < 0.01, *p < 0.01 compared to the control. (C) Immunofluorescence microscopy of E-cadherin and vimentin in human lung cancer CL1-0 and CL1-0-CR cells. Cells treated with AAE (500 μg/mL) for 48 h exhibited increased E-cadherin expression and decreased vimentin expression in all cell lines compared to those in the control cells. The panel presents E-cadherin (green), vimentin (red), 4′,6-diamidino-2-phenylindole (blue), and merged images (original magnification, × 200). Scale bar, 200 μm. The mean values were significantly different compared with the control group. *p < 0.05, **p < 0.01, ***p < 0.001 (D) Quantitative polymerase chain reaction analysis of E-cadherin, vimentin, and TJP-1 levels in CL1-0 and CL1-0-GR cells after treatment with AAE (500 μg) for 48 h. The relative concentrations of E-cadherin, vimentin, and TJP-1 of the vehicle control was shown in the graph. Data shown as the mean ± standard error of values obtained in at least three independent experiments, ***p < 0.001, **p < 0.01, *p < 0.05 compared with control cells. (For interpretation of the references to color in this figure legend, the reader is referred to the Web version of this article.)

0 and CL1-0-GR cells. AAE inhibited cell cloning ability of CL1-0 parent and CL1-0-GR cells in a dose-dependent manner (Fig. 3A). AAE suppressed the aggregation of both CL1-0 and CL1-0-GR cells. The area of the aggregated CL1-0 cells increased to 147%, and CL1-0-GR cells decreased to 74% after 500 μg of AAE treatment, respectively, compared to the control cells (100%). However, the density of cells was reduced to 24% and 35% for the CL1-0 and CL1-0-GR cells, respectively, compared to that in the control group (100%) (Fig. 3B). These findings show that AAE suppressed the aggregation, dramatically decreasing cell area and density of gemcitabine-resistant lung cancer cells.

3.4. AAE treatment decreases mitochondrial membrane potential and increases ROS production

Earlier studies reported that ethyl acetate extract of A. argyi inhibited the development of *Verticillium dahlia* by inducing the ROS production and downregulating the genes involved in the metabolic pathway (Wang et al., 2022). *Artemisia argyi* essential oil induced apoptosis through mitochondrial pathway; it decreases MMP and increases ROS production in *Candida albicans* (Shi et al., 2017). Because damage to the mitochondrial membrane leads to intrinsic apoptosis, we tested whether AAE has any impact on mitochondrial function in lung cancer cells. In the present study, AAE significantly decreased MMP polarization in CL1-0 cells by approximately 40% ($p < 0.01$) and 60% ($p < 0.001$) at doses of 300 and 500 μg for 48 h, respectively (Fig. 4C). In addition, AAE decreased MMP polarization in CL1-0-GR cells by 30% ($p < 0.05$) and 50% ($p < 0.01$) at doses of 300 and 500 μg for 48 h, respectively. Additionally, we tested if AAE increased ROS generation in the mitochondria of lung cancer cells. We found that AAE significantly increased the production of ROS (300 μg AAE: CL1-0: 5% $p < 0.05$, CL1-0-GR: 4% $p < 0.05$; CL1-0: 6% $p < 0.01$; 500 μg CL1-0-GR: 5% $p < 0.05$) (Fig. 4A). Because AAE significantly upregulates the ROS level, we speculate that AAE may inhibit enzymatic pathways that protect the cells against oxidative stress. Thus, we investigated anti-oxidant enzyme protein levels. We found that AAE treatment decreased protein levels of superoxide dismutase 1 (SOD-1) and catalase in CL1-0 and CL1-0-GR cells (Fig. 4B), consistent with the above result. These results suggest that the pro-apoptotic effects of AAE involve mitochondrial-mediated apoptotic pathways with both the depolarization of MMP and ROS generation in both CL1-0 and CL1-0-GR lung cancer cell lines.

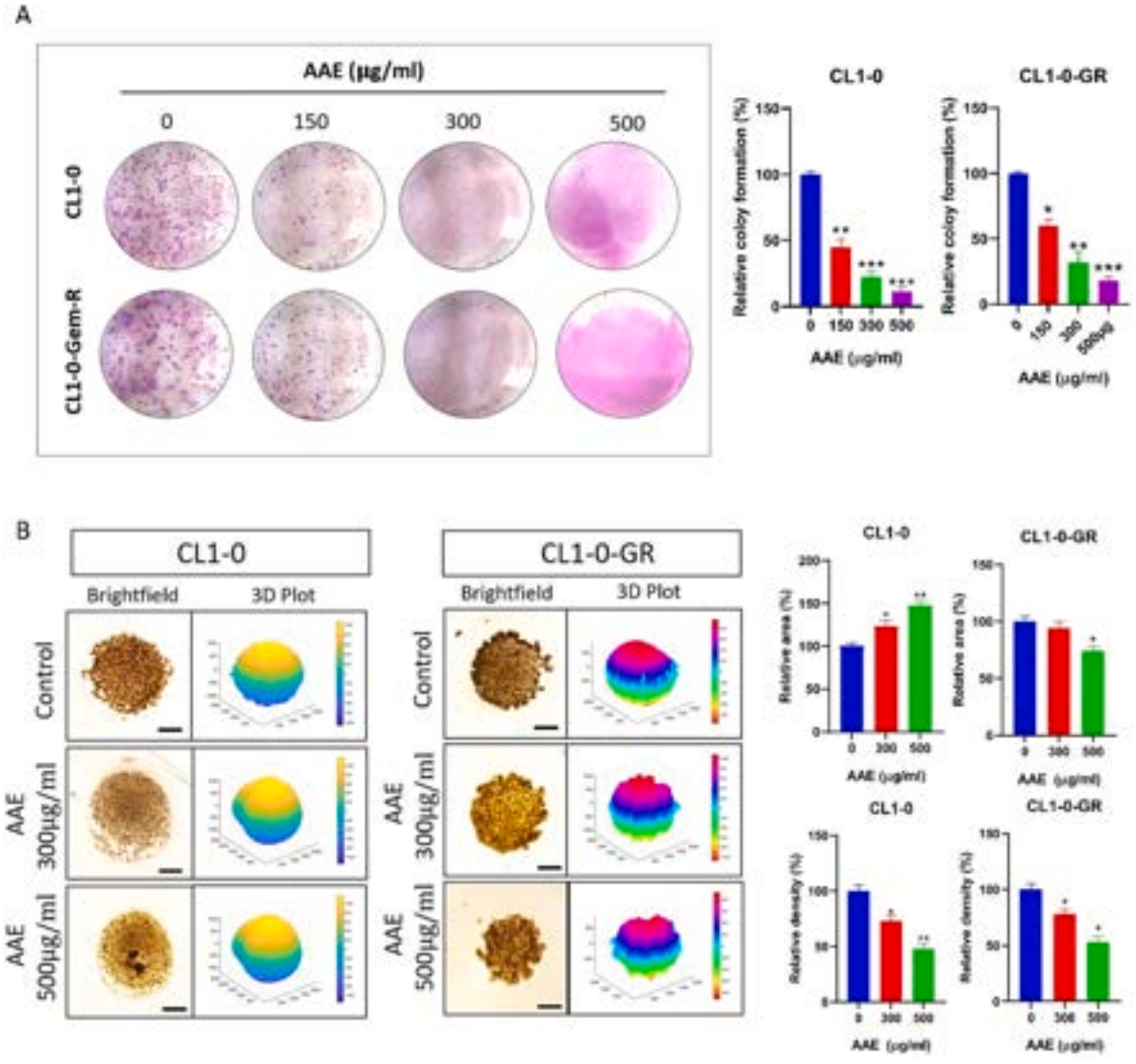

Fig. 3. Inhibition of cancer cell aggregation and colony formation by *Artemisia argyi* water extract (AAE) in CL1-0 parent and gemcitabine-resistant (CL1-0 GR) cells. (A) The colony formation of CL1-0 and CL1-0-GR cells was inhibited upon exposure to AAE. (B) Changes in the tumor spheroid morphology following AAE treatment were presented with bright-field images and 3D plots. Scale bar, 50 μm. The total area and density of the spheroid were calculated using ImageJ software. Scale bar indicates 100 μm. The asterisks indicate statistically significant differences compared to the control group (*$p < 0.05$; **$p < 0.01$; ***$p < 0.001$).

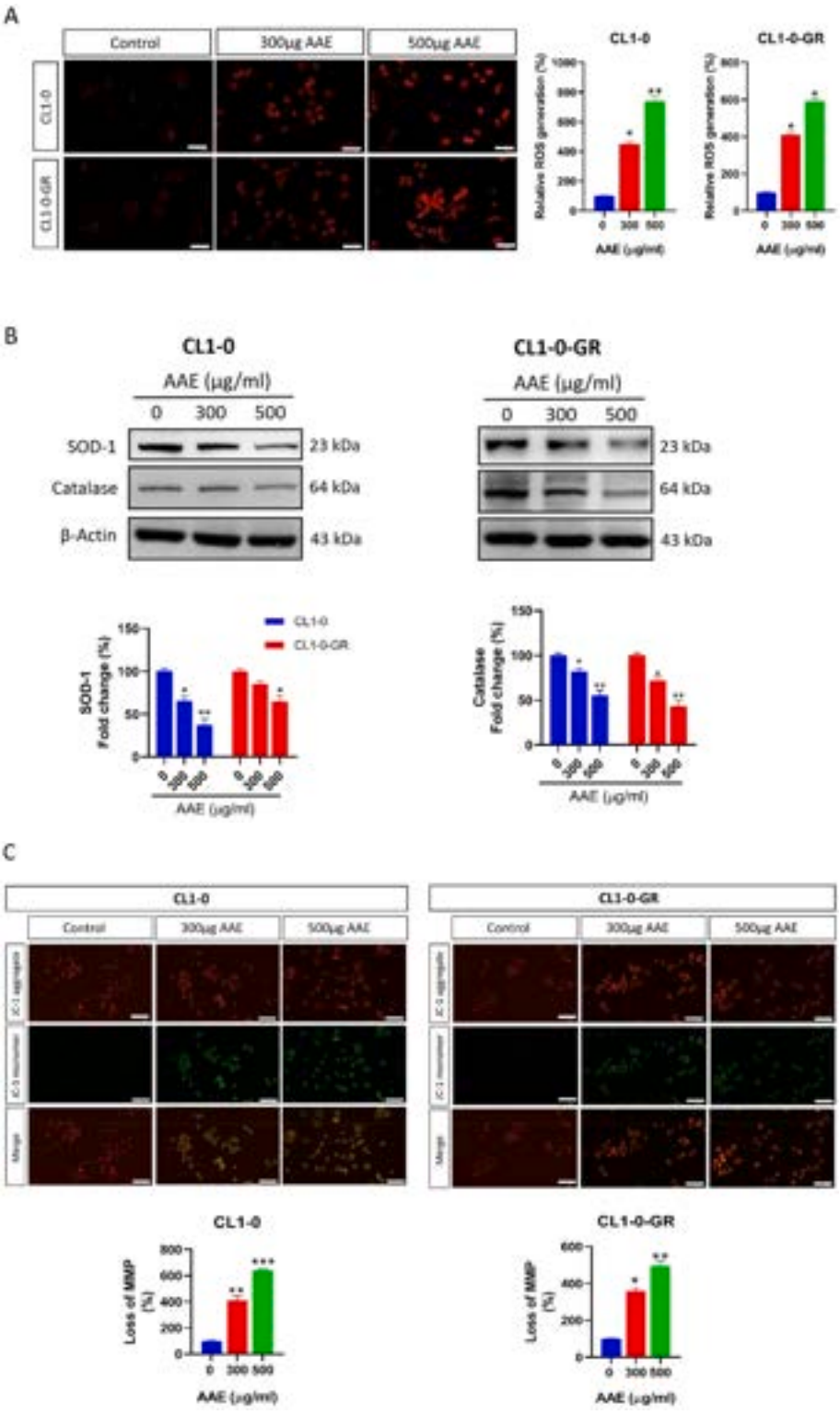

Fig. 4. Effect of *Artemisia argyi* water extract (AAE) on mitochondrial dysfunction and reactive oxygen species (ROS) production in lung cancer cells. (A) AAE-induced intracellular ROS production was estimated using MitoSOX Red. Mitochondrial ROS levels were analyzed using fluorescence microscopy and compared with those in untreated control cells. Scale bar, 100 μm. The mean values were significantly different compared with the control group. $*p < 0.05$, $**p < 0.01$, $***p < 0.001$ (B) CL1-0 and CL1-0-GE cells were treated with 300 and 500 μg of AAE for 48 h, and then the levels of the anti-oxidant enzymes SOD-1 and catalase were determined. Western blotting data were quantified by densitometry and ImageJ software, and normalized to GAPDH. $*p < 0.05$, $**p < 0.01$, $***p < 0.001$ compared with the untreated group (C) Immunofluorescence image analysis indicated MMP in CL1-0 and CL1-0-GR cells treated with AAE. The loss of MMP was analyzed using JC-1 red and green fluorescence ratios. Scale bar, 100 μm. Asterisks indicate a significant change after AAE treatment ($***p < 0.001$, $**p < 0.01$, $*p < 0.05$). (For interpretation of the references to color in this figure legend, the reader is referred to the Web version of this article.)

3.5. AAE increases apoptosis in lung cancer cells

Decreases in cell viability, ROS induction, and mitochondrial membrane polarization suggest that AAE may induce apoptosis. Thus, we measured the number of apoptotic cancer cells using Annexin V and PI staining following treatment with AAE (Fig. 5A). In both CL1-0 and CL1-0-GR cells, apoptosis was induced by AAE in a dose-dependent manner. In cells treated with 300 and 500 μg/mL AAE, the early-apoptosis population was increased by 2 and 2.8-fold in CL1-0 cells and 2.5 and 5-fold in CL1-0-GR cells, respectively, compared to the untreated control group. For late apoptosis, the percentage of cells increased 2.4 and 3.3-fold only in CL1-0 cells treated with 300 and 500 μg/mL AAE compared to the untreated control group. Furthermore, we used the TUNEL assay to measure AAE-induced apoptosis in CL1-0 and CL1-0-GR cells (Fig. 5B). DNA fragmentation was detected in the nuclei of both CL1-0 and CL1-0-GR cells undergoing apoptosis. To investigate this result further, we measured the expression of pro- and anti-apoptotic markers by western blotting following 300 and 500 μg/mL AAE treatment (Fig. 5C). AAE decreased Bcl-2 expression by 0.5-fold in both CL1-0 and CL1-0-GR cells; however, it increased the expression of both Bak (CL1-0: 1.45-fold; CL1-0-GR: 1.5-fold) and cleaved Caspase-3 (CL1-0: 1.4-fold; CL1-0-GR: 1.3-fold). These results indicate that AAE influences apoptotic signaling pathways in both CL1-0 and CL1-0-GR lung cancer cells.

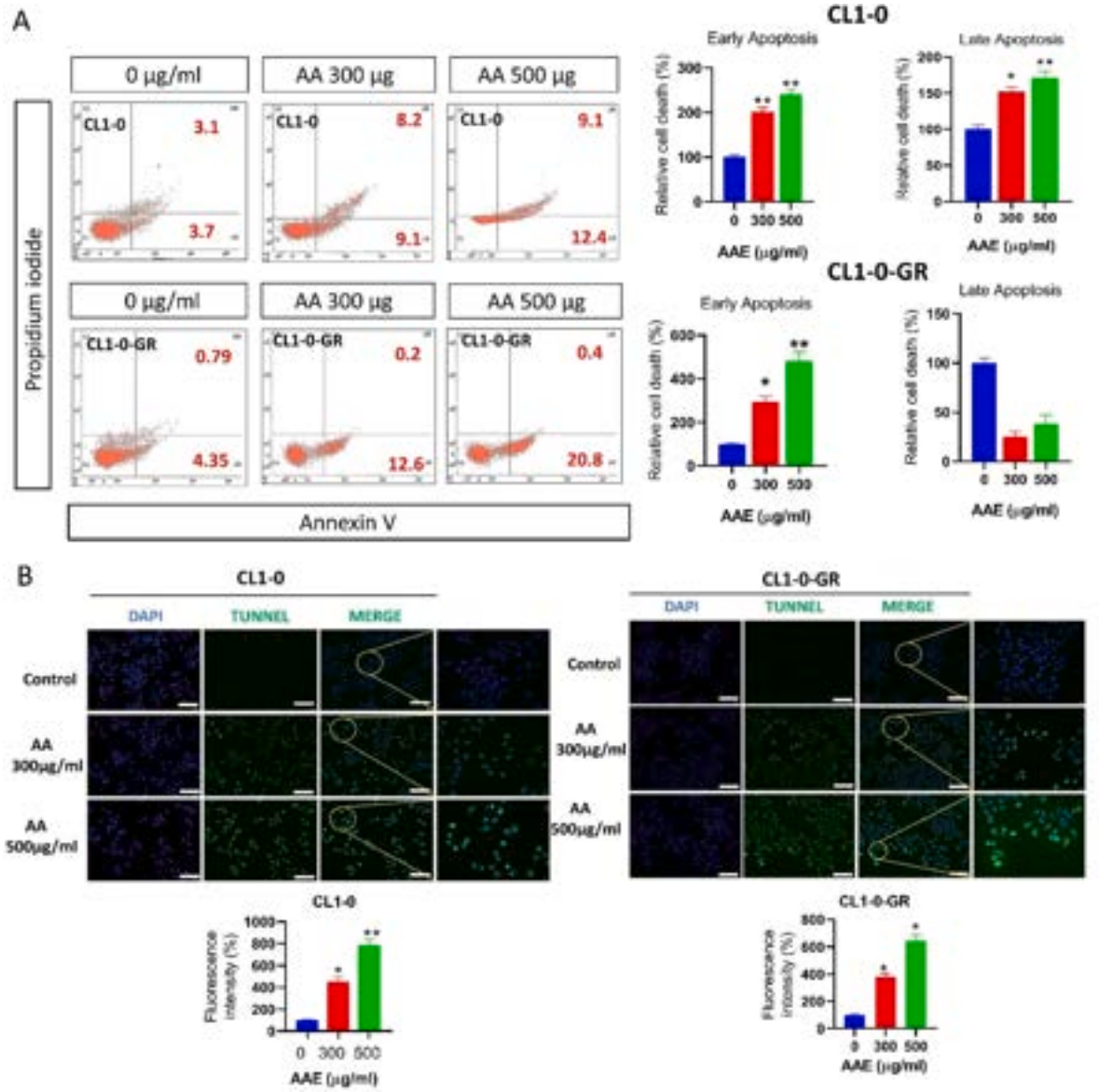

Fig. 5. *Artemisia argyi* water extract (AAE) induces apoptosis in CL1-0 parental and chemo-resistant (CL1-0-GR) lung cancer cells. (A) Flow cytometric detection of apoptosis in AAE-treated lung cancer cells. Annexin V stained late apoptotic cells, which showed dose-dependent effects of AAE at doses of 350 and 500 μg for 48 h. The percentages of cells in each quadrant indicate (upper left) necrotic cells, (lower left) live cells, (lower right) early apoptotic cells, and (upper right) late apoptotic cells. Data indicate the percentage of apoptotic cells (*$p < 0.05$, **$p < 0.01$, ***$p < 0.001$) compared with the nontreatment group. (B) Parental CL1-0 cells and CL1-0-GR cells were treated with AAE (10 μl/mL) for 48 h. TUNEL staining affirmed the presence of apoptotic cells, which were visualized by green fluorescence (left); the nucleus was stained by DAPI (middle, blue spots), and merged images were obtained (right side). Scale bar, 20 μm. The mean values were significantly different compared with the control group. *$p < 0.05$, **$p < 0.01$, ***$p < 0.001$ (C) CL1-0 and CL1-0-GE cells were treated with 300 μg and 500 μg of AAE for 48 h, and then the levels of apoptosis-related proteins (c-Caspase-3/Caspase-3, Bak, and Bcl-2) were determined by western blotting. Western blotting data were quantified by densitometry and ImageJ software, and normalized to GAPDH. (*$p < 0.05$, **$p < 0.01$, ***$p < 0.001$ compared with the control group). (For interpretation of the references to color in this figure legend, the reader is referred to the Web version of this article.)

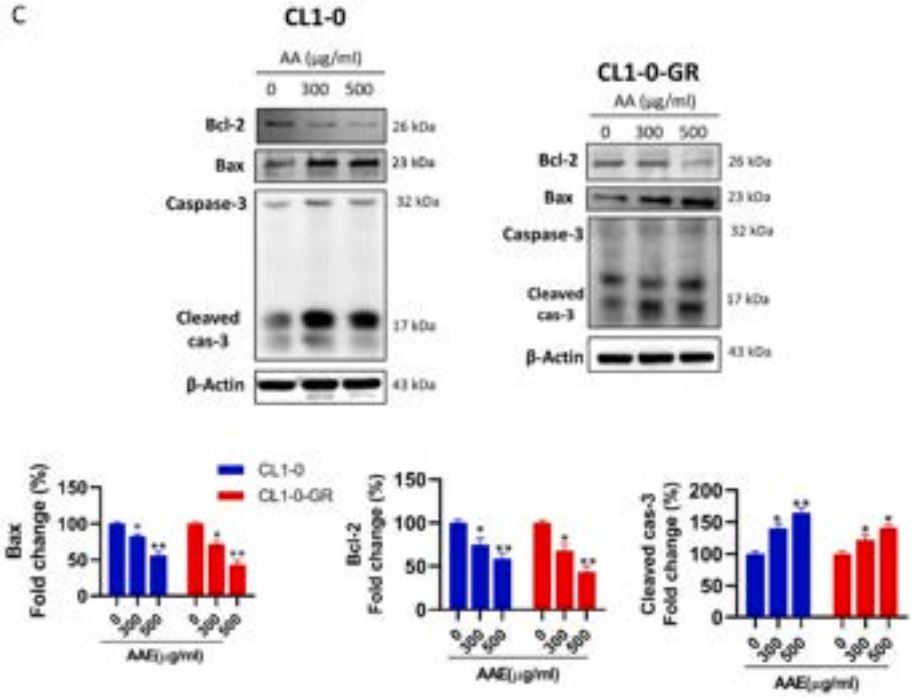

Fig. 5. (*continued*).

3.6. AAE inactivates the PI3K/MAPK intracellular signaling pathways

It has been reported that *Artemisia argyi* Folium extract inhibited 2,4-dinitrochlorobenzene induced phosphorylation of MAPK (ERK, JNK), PI3K/AKT, and IκBα (Han et al., 2016). Furthermore, *Artemisia argyi* treatment inhibits T cell proliferation by suppressing NFAT and NF-κB transcription (Zimmermann-Klemd et al., 2020). Thus, we aimed to examine the molecular mechanisms involved in the pro-apoptotic effect of AAE in CL1-0 and CL1-0-GR cells using western blot analysis. Cells were treated with AAE (0 μg, 300 μg, 500 μg) for 48 h and evaluated for PI3K/AKT and MAPK, which are involved in cell proliferation and survival. In both CL1-0 and CL1-0-GR cells, phosphorylation of AKT was significantly reduced (CL1-0: up to 0.3-fold, $p < 0.01$; CL1-0-GR: up to 0.5-fold, $p < 0.05$) compared to that in the untreated control group (Fig. 6A). In addition, AAE treatment suppressed ERK1/2 phosphorylation (CL1-0: up to 0.6-fold, $p < 0.05$; CL1-0-GR: up to 0.7-fold, $p < 0.05$) and p-JNK (CL1-0: up to 0.2-fold, $p < 0.01$; CL1-0-GR: up to 0.5-fold, $p < 0.05$) in both cell lines compared to controls (Fig. 6B). These results suggest that AAE negatively regulates the PI3K/AKT and MAPK signaling pathways in CL1-0 and CL1-0-GR cells.

3.7. Synergistic effects of AAE and chemotherapeutic drugs

We investigated the synergistic anti-cancer effects of AAE and doxorubicin, oxaliplatin, irinotecan, and gemcitabine using the MTT assay. Cells were incubated with AAE (250 μg) alone or co-treated with doxorubicin (DOX, 2.5 μM), oxaliplatin (OXA, 5 μM), irinotecan (CPT-11, 5 μM), or gemcitabine (Gem, 12.5 μM). The combination of AAE with chemotherapy drugs significantly ($P < 0.05$) attenuated CL1-0 viability (Fig. 7A). Furthermore, combination AAE treatment with anti-cancer drugs further inhibited 3D spheroid formation in CL1-0 cells. Notably, AAE reduced the total spheroid density when combined with doxorubicin and irinotecan from 49% to 24% ($p < 0.001$) and from 53% to 31% ($p < 0.01$), respectively (Fig. 7B). CL1-0-GR cell viability was evaluated using gemcitabine with or without AAE. The combination of AAE and increasing concentrations of gemcitabine (5, 10, 20, 30 μM) decreased the viability of CL1-0-GR cells (Fig. 7C). Our results suggest that AAE enhances the effect of the standard anti-cancer drug by mediating combinational effects in lung cancer cells (see Fig. 8).

4. Discussion

Recent studies have attempted to discover and develop natural products with anti-cancer properties. Extracts from *Artemisia* species exhibit strong antitumor properties without increasing the risk of chemotherapy resistance. *Artemisia argyi* is a TCM herb that exerts numerous pharmacological effects. Studies have shown that AAE inhibits several types of cancer, such as colon cancer (Jeung-Min et al., 2010), hepatocellular carcinoma (Li et al., 2021), cervical cancer (Lee et al., 2005), and gastric cancer (Zhang et al., 2018). Jaceosidin, a flavone in *A. argyi*, induces cell cycle arrest, ROS, diminished mitochondrial membrane potential, the release of cytochrome *c*, and activation of caspase 3 in glioblastoma cells (Khan et al., 2012). Moreover, Artemisinin B, isolated from AAE, induces cell cycle arrest and apoptosis in breast cancer cells. Combining antitumor agents with herbal medicine is a potential strategy for improving chemotherapy's effect on cancer cells (Xue et al., 2017). In a clinical trial, gemcitabine combined with carboplatin showed reduced toxicity and increased efficacy in advanced non-small-cell lung cancer (Zatloukal and Petruzelka, 2002). Nevertheless, potency is frequently reduced by tumors developing drug resistance. Therefore, alternative cancer therapies are required. This study aimed both to evaluate the apoptotic and additive effects of AAE in gemcitabine-resistant lung cancer cells and to elucidate the molecular mechanisms and signaling pathways involved.

Herbal medicines can individually or synergistically enhance the antitumor activity of some types of cancer cells. For example, Xiao-Fan et al. found that the combination of *Juniperus indica* Bertol extract and cisplatin enhanced apoptosis of melanoma cells through disrupting AKT/MAPK signaling (Huang et al., 2021). Meng-ping et al. discovered that *Sanguisorba officinalis* enhanced 5-fluorouracil cytotoxicity in colorectal cancer cells (Liu et al., 2016). In addition, extracts of *Berberis aristata* root and *Azadirachta indica* seed induced cytotoxicity in cisplatin-resistant osteosarcoma cells (Sengupta et al., 2017). Similarly, our study demonstrated that AAE inhibited cell viability, proliferation, and induced apoptosis in gemcitabine-resistant CL1-0 cells in a concentration-dependent manner. CL1-0 parent cells served as a

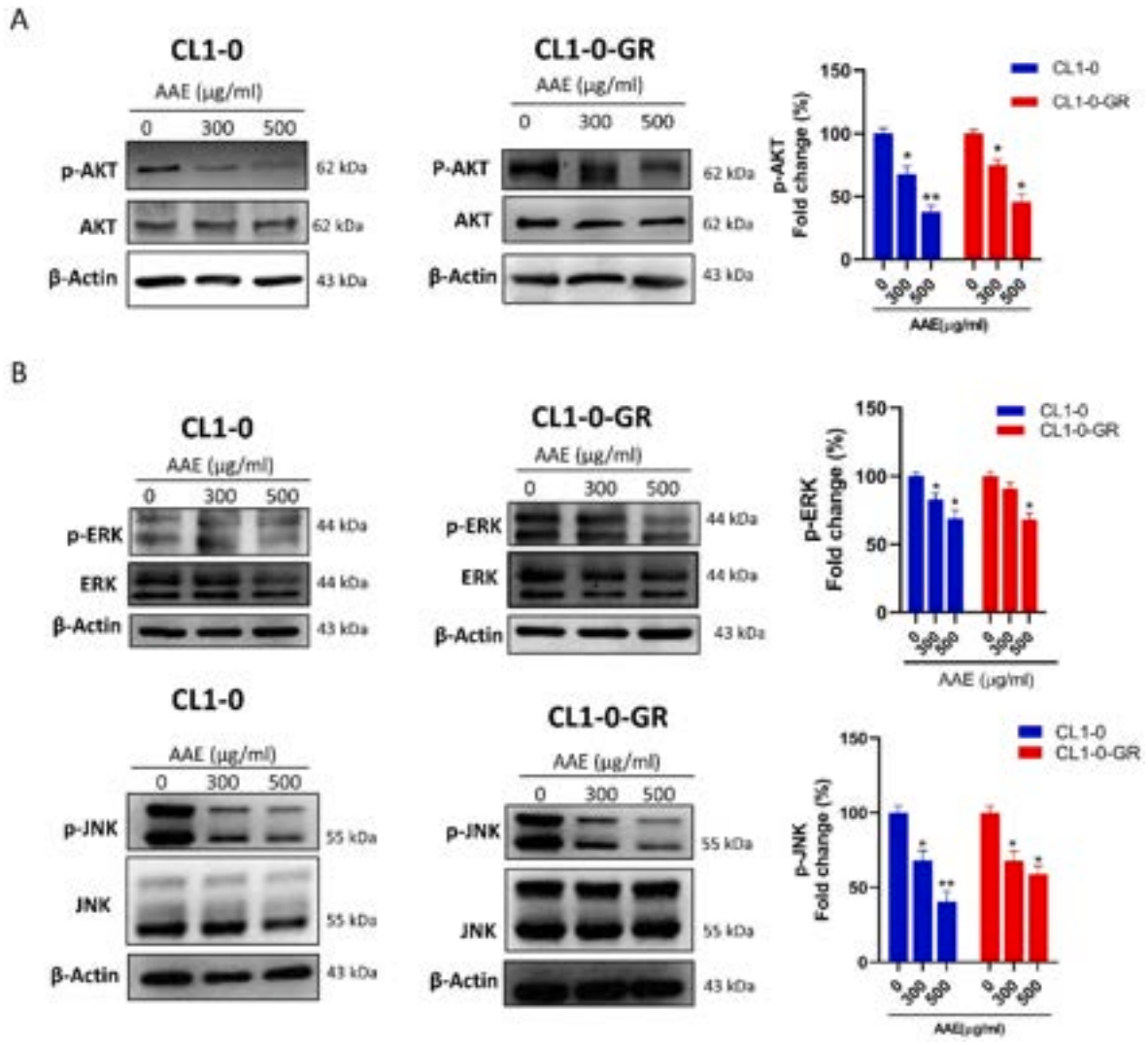

Fig. 6. Effects of *Artemisia argyi* water extract (AAE) on cell signaling molecules in CL1-0 and CL1-0-GR lung cancer cells. Dose-dependent changes in the phosphorylation of (A) AKT, (B) ERK and JNK proteins in response to AAE at doses of 300 μg or 500 μg were determined by western blotting. Dose-dependent effects of AAE on the phosphorylation of targeted signaling molecules presented relative to those in non-treated control cells. The data are from three independent experiments (***P < 0.001, **P < 0.01, and *P < 0.05).

comparison with gemcitabine-resistant (CL1-0-GR) cells to show how similar cells respond to AAE treatment in absence of acquired resistance.

Abnormally activated cell migration and invasion programs promote lung cancer cell metastases to adjacent tissues, blood vessels, and organs, and is associated with poor prognosis and high mortality rates (Fares et al., 2020). Vimentin, a marker for EMT, is a type III intermediate filament protein responsible for cell migration, adhesion, and motility. During EMT process, vimentin expression increases and is stabilized by the downregulation of E-cadherin (Carneiro and El-Deiry, 2020). Tight junction protein 1 (TJP1) is overexpressed and promotes invasion with N-cadherin (Lee et al., 2015). However, other researchers have investigated whether natural products can disrupt EMT. Li et al. showed that *A. arygi* essential oil treatment inhibits cell proliferation, metastasis, and EMT by suppressing the oncoantigen DEPDC1 and blocking the cell cycle in the G2/M phase in hepatocellular carcinoma (Li et al., 2021). Tseng et al. found that the polysaccharide-containing fraction from AAE blocked the interaction of podoplanin and C-type lectin receptor 2, which inhibits tumor cell invasion and metastasis (Tseng et al., 2020). Consistent with those findings, we report that AAE treatment suppressed cancer cell proliferation, invasion, and migration and reduced EMT marker expression in the CL1-0 and CL1-0-GR cells. Similarly, the mRNA expression of vimentin and TJP-1 was downregulated by AAE. These findings suggest that AAE inhibited proliferation, invasion, and migration of lung cancer cells through downregulating the vimentin, TJP-1, and PCNA expression. In cancer research, spheroid formation is a convenient model to analyze the 3D morphological difference *in vitro* (Pinto et al., 2020). AAE treatment was found to inhibit the aggregation of lung cancer cells, demonstrating that AAE inhibits lung cancer cell line growth.

MMP depolarization leads to the activation of pro-apoptotic proteins, alteration of mitochondrial function, which then activates the early stages of programmed cell death. The MMP is essential for Ca^{2+} uptake, ROS stress, and ATP biosynthesis (Weinberg and Chandel, 2015). The constituents of *A. argyi* may induce intracellular ROS production, cell cycle arrest, Caspase-dependent apoptosis, and activate NADPH oxidase in gastric carcinoma cells (Zhang et al., 2018). ROS production is crucial for cell growth and survival; however, excessive ROS levels lead to cell death. Uncontrolled ROS levels in cells induce cell death via intrinsic apoptotic signals in the mitochondria (Reczek and Chandel, 2017). Therefore, mitochondrial membrane depolarization is a suitable indicator of mitochondrial-initiated apoptotic status. In our study, we found AAE treatment depolarized the mitochondrial membrane. Decreased MMP causes a decrease in Bcl-2 expression and initiates the caspase cascade, leading to apoptosis(Wang and Welsh, 2014). Activation of

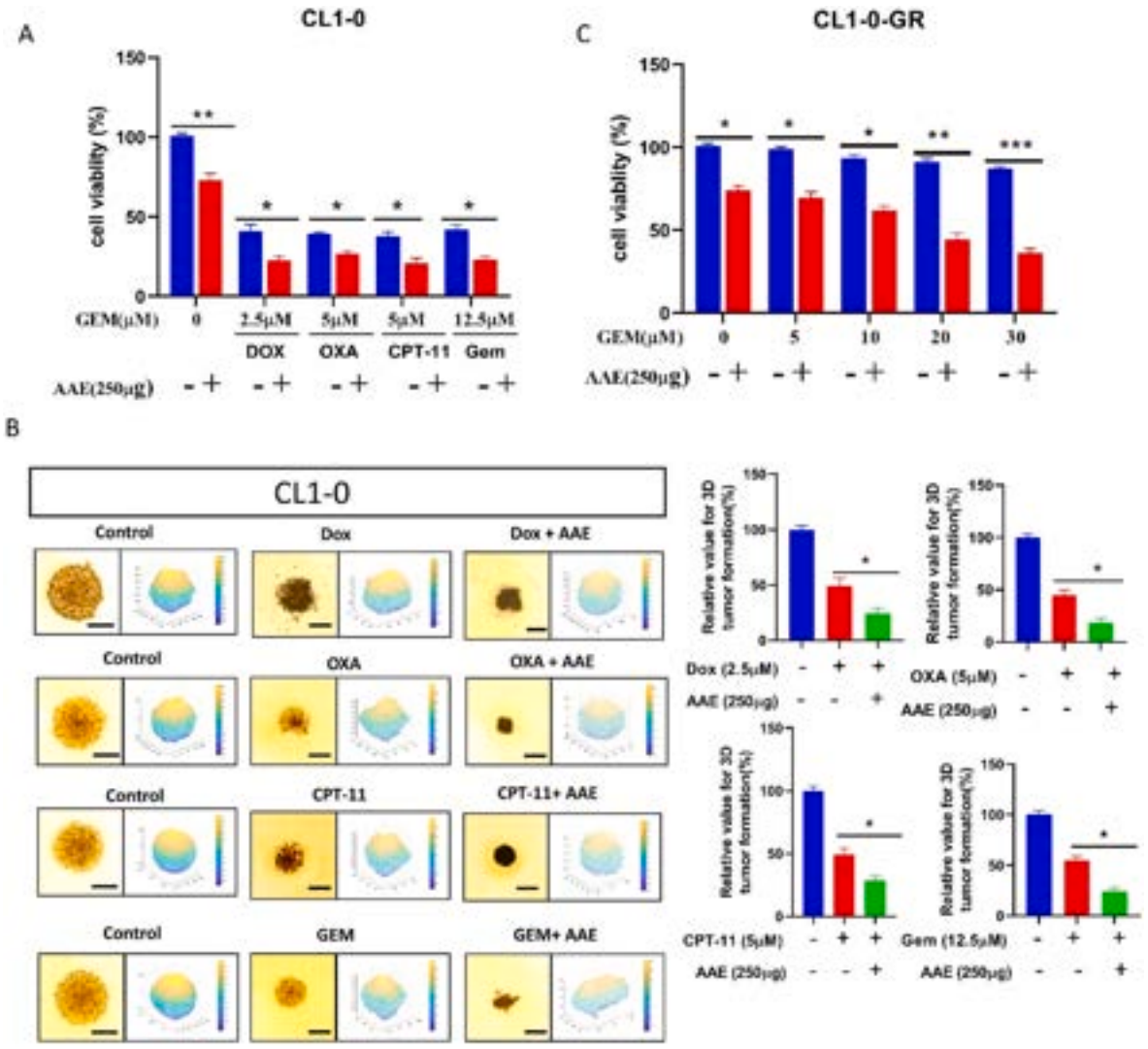

Fig. 7. ***Artemisia argyi*** **water extract (AAE) acts synergistically with standard anticancer drugs on lung cancer cells**. (A) The effects of AAE combined with doxorubicin, oxaliplatin, irinotecan (CPT-11), and gemcitabine on cell viability. (B) Bright-field images show the changes in spheroid morphology following AAE treatment combined with doxorubicin, oxaliplatin, irinotecan (CPT-11), and gemcitabine. The scale bar indicates 100 μM. (C) Cell viability detection of CL1-0-GR cells in response to the combination of gemcitabine and AAE using the MTT assay. Asterisks indicate a significant change after AAE treatment (***$p < 0.001$, **$p < 0.01$, *$p < 0.05$).

caspase-9 and -8 shows the involvement of both intrinsic and extrinsic apoptotic pathways that consecutively lead to caspase-3 activation (Huang et al., 2014). We discovered that AAE treatment significantly decreased Bcl-2 and caspase activity. Additionally, we found that cleaved caspase-3 expression was high, indicating activation of apoptotic pathways, likely contributing to the apoptosis of CL1-0 cells. Similar results were observed in the AAE-treated CL1-0-GR cells.

Apoptotic resistance prevents programmed cell death in cancer cells, which can lead to drug resistance; therefore, new treatments are necessary to induce apoptosis (Mohammad et al., 2015). In the present study, AAE treatment significantly decreased cell viability and induced apoptosis in the CR1-0-GR cells. Although AAE exposure in the parent cells showed a more significant inhibitory effect than in gemcitabine-resistant cells, these results indicate that AAE induced apoptosis and sensitized gemcitabine-resistant lung cancer cells to apoptotic triggers. These findings suggest that AAE can work additively with gemcitabine even in lung cancer cells resistant to gemcitabine. In addition, we evaluated AAE's effect on apoptosis activity using Annexin V staining. In CL1-0 cells, AAE induced late apoptosis (A + PI+), whereas, in CL1-0-GR cells, AAE induced early apoptosis (A + PI-) (Khazaei et al., 2017). Therefore, in 48 h, AAE may dramatically damage the phospholipid assembly associated with nuclear membrane integrity in parent cells; meanwhile, in gemcitabine-resistant cells, AAE may attenuate only the phospholipid assembly.

The intercellular signaling mechanisms underlying the chemotherapeutic effect of AAE are not well understood. The MEK/ERK and PI3K/AKT pathways control fundamental physiological processes, such as differentiation, cell proliferation, cytoskeleton organization, cell metabolism, cell death, and survival (Guo et al., 2020; Porta et al., 2014). Constitutive activation of these signaling pathways is a hallmark of cancer, and dysregulation of these pathways, either genetic or epigenetic, contributes to the initiation, progression, and metastasis of lung cancers (Cheng et al., 2014; Salaroglio et al., 2019). The activation of AKT and ERK signaling enables intrinsic resistance of tumor cells to EGFR inhibitors (Li et al., 2011). A previous study has shown that AKT and ERK inhibition partially enhanced the chemosensitivity of gefitinib-resistant lung cancer (Li et al., 2020). Similarly, in our study, we found that phosphorylation of AKT, ERK and JNK was down-regulated by AAE treatment, suggesting that AAE may affect, at least to some extent, the regulation of the AKT/ERK pathway. However, further

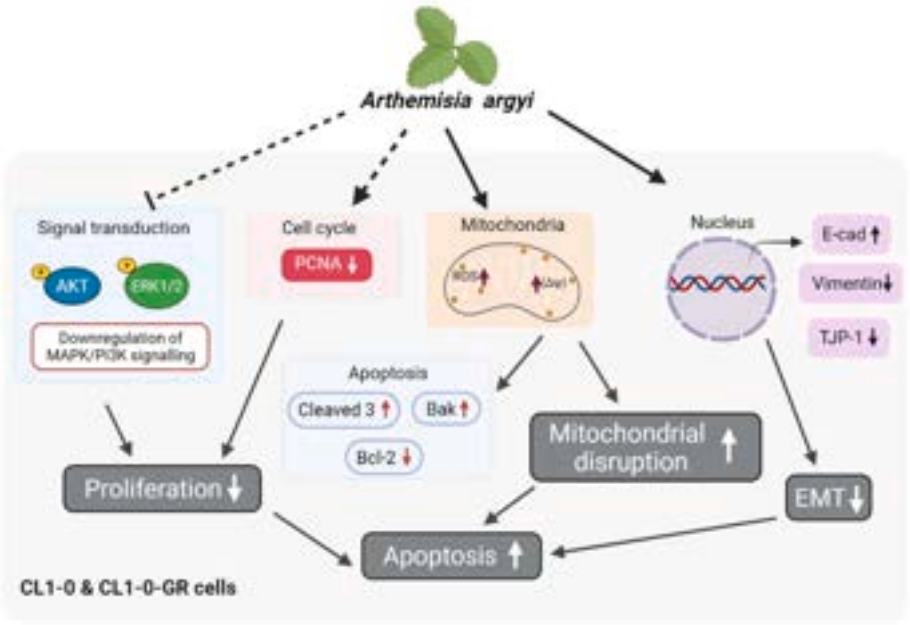

Fig. 8. *Artemisia argyi* water extract (AAE) targets PI3K/AKT and MAPK signaling pathways. Anticancer mechanisms regulated by *Artemisia argyi* water extract (AAE), targeting the survival and proliferation pathways in CL1-0 parent and CL1-0-GR cells. AAE inhibits PI3K/AKT and MAPK signaling by downregulating the phosphorylation of AKT and ERK1/2. In addition, AAE activates the intrinsic apoptosis pathway by inducing reactive oxygen species production and mitochondrial membrane potential.

investigations are required to confirm the present findings.

Herbal extracts may increase the efficacy of anticancer drugs (Woo et al., 2017). However, there have been no reports on AAE extracts, although their derivatives can increase the sensitivity of lung cancer cells to commercial anticancer agents (Lee et al., 2020). This study is the first to demonstrate that AAE may act synergistically with anticancer drugs. Compared to treatment with AAE only, combination treatments, including AAE and doxorubicin, irinotecan, or gemcitabine, significantly decreased the viability and aggregation of lung cancer cells. These findings suggest that AAE may mitigate the risk of gemcitabine resistance and inhibit the viability of gemcitabine-resistant lung cancer cells. This effect was comparable to that observed in gemcitabine-resistant pancreatic cancers (Pak et al., 2016). Sustaining mitochondrial activity is necessary to maintain the sensitivity of lung cancer cells to conventional chemotherapy agents. These findings suggest that mitochondrial dysfunction triggered by exposure to AAE may help boost the sensitivity of lung cancer cells to chemotherapeutic drugs. In addition, AAE-mediated oxidative stress and changes in cellular pathways may contribute to the increased chemosensitivity of lung cancer cells.

5. Conclusion

In this study, we discovered the anti-cancer effect of *A. argyi* on lung cancer cells and its underlying mechanisms of action. AAE was associated with increased cell apoptosis and decreased invasion, migration, and EMT in parental and chemo-resistant CL1-0 lung cancer cells. Furthermore, AAE impairs mitochondrial membrane function and induces ROS generation in the treated cells. Its mechanism may involve the PI3K/AKT and MAPK signaling pathways. These findings provide molecular insights into the anti-tumor activity of *A. argyi* and suggest that it may be a candidate for adjuvant therapy in lung cancer treatment.

Ethics approval and consent to participate

Not applicable.

Consent for publication

All authors have provided consent for publication of the manuscript in the journal of Chinese Medicine.

Availability of data and materials

This publication contains all of the data produced or analyzed during this project.

Funding number

IMAR-109-01-04-06 (Hualien Tzu Chi Hospital)

CMU107-ASIA-08, CMU108-MF-64 (China Medical University and ASIA University)

CRediT authorship contribution statement

San-Hua Su: Conceptualization, Data curation, Formal analysis, Funding acquisition, Investigation. **Navaneethan Sundhar:** Data curation, Formal analysis, Investigation, Methodology, Writing – original draft, Writing – review & editing. **Wei-Wen Kuo:** Supervision, Validation, Visualization. **Shang-Chih Lai:** Supervision, Validation, Visualization. **Chia-Hua Kuo:** Supervision, Validation, Visualization. **Tsung-Jung Ho:** Supervision, Validation, Visualization. **Pi-Yu Lin:** Project administration, Resources, Software. **Shinn-Zong Lin:** Project administration, Resources, Software. **Cheng Yen Shih:** Project administration, Resources, Software. **Yu-Jung Lin:** Conceptualization, Data curation, Investigation, Project administration, Resources, Supervision, Validation. **Chih-Yang Huang:** Conceptualization, Data curation, Funding acquisition, Investigation, Project administration, Resources, Supervision, Validation, All data were generated in-house, and no paper mill was used. All authors agree to be accountable for all aspects of this work ensuring its integrity and accuracy.

Declaration of competing interest

The authors had no conflict of interests to declare.

Data availability

The authors do not have permission to share data.

Acknowledgments

We would like to acknowledge the core facilities provided by

Advanced Instrumentation Centre of Department of Medicine Research, Hualien Tzu Chi Hospital, Buddhist Tzu Chi Medical Foundation, Hualien, Taiwan.

Abbreviations:

AAE	Artemisia argyi extract
AKT	Protein kinase B
Bcl2	B-cell lymphoma 2
Bak	Bcl-2-associated-X protein
ERK	extracellular signal-regulated kinases
GR	Gemcitabine resistance
MMP	Mitochondrial membrane potential
ROS	Reactive oxygen species
SOD-1	superoxide dismutase 1
ABCC10	ATP-binding cassette (ABC) transporter C10
CYP3A5	Cytochrome P450 Family 3 Subfamily A Member 5

References

Ardalani, H., Avan, A., Ghayour-Mobarhan, M., 2017. Podophyllotoxin: a novel potential natural anticancer agent. Avicenna J. Phytomed. 7 (4), 285–294.

Carneiro, B.A., El-Deiry, W.S., 2020. Targeting apoptosis in cancer therapy. Nat. Rev. Clin. Oncol. 17 (7), 395–417.

Cheng, H., Shcherba, M., Pendurti, G., Liang, Y., Piperdi, B., Perez-Soler, R., 2014. Targeting the PI3K/AKT/mTOR pathway: potential for lung cancer treatment. Lung Cancer Manag. 3 (1), 67–75.

Chinese Pharmacopoeia Commission, 2015. In: Chinese Pharmacopoeia Commission (Ed.), The Pharmacopoeia of the People's Republic of China 2015 Edition, , 10th1. Chinese Pharmacopoeia Commission, Beijing.

Choi, E., Kim, G., 2013. Effect of artemisia species on cellular proliferation and apoptosis in human breast cancer cells via estrogen receptor-related pathway. J. Tradit. Chin. Med. 33 (5), 658–663.

Chu, Y.W., Yang, P.C., Yang, S.C., Shyu, Y.C., Hendrix, M.J., Wu, R., Wu, C.W., 1997. Selection of invasive and metastatic subpopulations from a human lung adenocarcinoma cell line. Am. J. Respir. Cell Mol. Biol. 17 (3), 353–360.

Dhanapal, A.C.T.A., Ming, T.W., Aung, H.P., Hao, S.J., 2016. Preliminary Screening of Artemisia Argyi for Antioxidant Potentials, 8, pp. 347–355.

Fares, J., Fares, M., Khachfe, H., Salhab, H., Fares, Y., 2020. Molecular principles of metastasis: a hallmark of cancer revisited. Signal Transduct. Targeted Ther. 5, 28.

Guo, Y.J., Pan, W.W., Liu, S.B., Shen, Z.F., Xu, Y., Hu, L.L., 2020. ERK/MAPK signalling pathway and tumorigenesis. Exp. Ther. Med. 19 (3), 1997–2007.

Hahm, K.B., Kim, J.H., You, B.M., Kim, Y.S., Cho, S.W., Yim, H., Ahn, B.O., Kim, W.B., 1998. Induction of apoptosis with an extract of Artemisia asiatica attenuates the severity of cerulein-induced pancreatitis in rats. Pancreas 17 (2), 153–157.

Han, H.M., Kim, S.J., Kim, J.S., Kim, B.H., Lee, H.W., Lee, Y.T., Kang, K.H., 2016. Ameliorative effects of Artemisia argyi Folium extract on 2,4dinitrochlorobenzeneinduced atopic dermatitislike lesions in BALB/c mice. Mol. Med. Rep. 14 (4), 3206–3214.

Hryciuk, B., Szymanowski, B., Romanowska, A., Salt, E., Wasag, B., Grala, B., Jassem, J., Duchnowska, R., 2018. Severe acute toxicity following gemcitabine administration: a report of four cases with cytidine deaminase polymorphisms evaluation. Oncol. Lett. 15 (2), 1912–1916.

Hsu, H.H., Kuo, W.W., Shih, H.N., Cheng, S.F., Yang, C.K., Chen, M.C., Tu, C.C., Viswanadha, V.P., Liao, P.H., Huang, C.Y., 2019. FOXC1 regulation of miR-31-5p confers oxaliplatin resistance by targeting LATS2 in colorectal cancer. Cancers 11 (10).

Huang, C.Y., Kuo, W.W., Yeh, Y.L., Ho, T.J., Lin, J.Y., Lin, D.Y., Chu, C.H., Tsai, F.J., Tsai, C.H., Huang, C.Y., 2014. ANG II promotes IGF-IIR expression and cardiomyocyte apoptosis by inhibiting HSF1 via JNK activation and SIRT1 degradation. Cell Death Differ. 21 (8), 1262–1274.

Huang, H.C., Wang, H.F., Yih, K.H., Chang, L.Z., Chang, T.M., 2012. Dual bioactivities of essential oil extracted from the leaves of Artemisia argyi as an antimelanogenic versus antioxidant agent and chemical composition analysis by GC/MS. Int. J. Mol. Sci. 13 (11), 14679–14697.

Huang, X.F., Gao, H.W., Lee, S.C., Chang, K.F., Tang, L.T., Tsai, N.M., 2021. Juniperus indica Bertol. extract synergized with cisplatin against melanoma cells via the suppression of AKT/mTOR and MAPK signaling and induction of cell apoptosis. Int. J. Med. Sci. 18 (1), 157–168.

Ikeda, R., Vermeulen, L.C., Lau, E., Jiang, Z., Sachidanandam, K., Yamada, K., Kolesar, J. M., 2011. Isolation and characterization of gemcitabine-resistant human non-small cell lung cancer A549 cells. Int. J. Oncol. 38 (2), 513–519.

Jeung-Min, L., Hyun-Jung, K., Seong-Hee, M., Hae-Ryong, P., 2010. Anticancer activity of artemisia argyi extracts on HT-29 human colon cancer cells. J. Cancer Prev. 15 (1), 76–82.

Kannathasan, T., Kuo, W.W., Chen, M.C., Viswanadha, V.P., Shen, C.Y., Tu, C.C., Yeh, Y. L., Bharath, M., Shibu, M.A., Huang, C.Y., 2020. Chemoresistance-associated silencing of miR-4454 promotes colorectal cancer aggression through the GNL3L and NF-kappaB pathway. Cancers 12 (5).

Khan, M., Yu, B., Rasul, A., Al Shawi, A., Yi, F., Yang, H., Ma, T., 2012. Jaceosidin induces apoptosis in U87 glioblastoma cells through G2/M phase Arrest. Evid. Based Complement. Alternat. Med. 2012, 703034.

Khazaei, S., Esa, N.M., Ramachandran, V., Hamid, R.A., Pandurangan, A.K., Etemad, A., Ismail, P., 2017. In vitro antiproliferative and apoptosis inducing effect of allium atroviolaceum bulb extract on breast, cervical, and liver cancer cells. Front. Pharmacol. 8, 5.

Lee, H.G., Yu, K.A., Oh, W.K., Baeg, T.W., Oh, H.C., Ahn, J.S., Jang, W.C., Kim, J.W., Lim, J.S., Choe, Y.K., Yoon, D.Y., 2005. Inhibitory effect of jaceosidin isolated from Artemisiaargyi on the function of E6 and E7 oncoproteins of HPV 16. J. Ethnopharmacol. 98 (3), 339–343.

Lee, J.Y., Bae, H., Yang, C., Park, S., Youn, B.S., Kim, H.S., Song, G., Lim, W., 2020. Eupatilin promotes cell death by calcium influx through ER-mitochondria Axis with SERPINB11 inhibition in epithelial ovarian cancer. Cancers 12 (6).

Lee, S.H., Paek, A.R., Yoon, K., Kim, S.H., Lee, S.Y., You, H.J., 2015. Tight junction protein 1 is regulated by transforming growth factor-beta and contributes to cell motility in NSCLC cells. BMB Rep. 48 (2), 115–120.

Li, H., Schmid-Bindert, G., Wang, D., Zhao, Y., Yang, X., Su, B., Zhou, C., 2011. Blocking the PI3K/AKT and MEK/ERK signaling pathways can overcome gefitinib-resistance in non-small cell lung cancer cell lines. Adv. Med. Sci. 56 (2), 275–284.

Li, N., Mao, Y., Deng, C., Zhang, X., 2008. Separation and identification of volatile constituents in Artemisia argyi flowers by GC-MS with SPME and steam distillation. J. Chromatogr. Sci. 46 (5), 401–405.

Li, S., Zhou, S., Yang, W., Meng, D., 2018. Gastro-protective effect of edible plant Artemisia argyi in ethanol-induced rats via normalizing inflammatory responses and oxidative stress. J. Ethnopharmacol. 214, 207–217.

Li, Y., Tian, Y., Zhong, W., Wang, N., Wang, Y., Zhang, Y., Zhang, Z., Li, J., Ma, F., Zhao, Z., Peng, Y., 2021. Artemisia argyi essential oil inhibits hepatocellular carcinoma metastasis via suppression of DEPDC1 dependent wnt/beta-catenin signaling pathway. Front. Cell Dev. Biol. 9, 664791.

Li, Y., Zang, H., Qian, G., Owonikoko, T.K., Ramalingam, S.R., Sun, S.Y., 2020. ERK inhibition effectively overcomes acquired resistance of epidermal growth factor receptor-mutant non-small cell lung cancer cells to osimertinib. Cancer 126 (6), 1339–1350.

Liu, M.P., Liao, M., Dai, C., Chen, J.F., Yang, C.J., Liu, M., Chen, Z.G., Yao, M.C., 2016. Sanguisorba officinalis L synergistically enhanced 5-fluorouracil cytotoxicity in colorectal cancer cells by promoting a reactive oxygen species-mediated, mitochondria-caspase-dependent apoptotic pathway. Sci. Rep. 6, 34245.

Liu, Y., He, Y., Wang, F., Xu, R., Yang, M., Ci, Z., Wu, Z., Zhang, D., Lin, J., 2021. From longevity grass to contemporary soft gold: explore the chemical constituents, pharmacology, and toxicology of Artemisia argyi H.Lev. & vaniot essential oil. J. Ethnopharmacol. 279, 114404.

Mohammad, R.M., Muqbil, I., Lowe, L., Yedjou, C., Hsu, H.Y., Lin, L.T., Siegelin, M.D., Fimognari, C., Kumar, N.B., Dou, Q.P., Yang, H., Samadi, A.K., Russo, G.L., Spagnuolo, C., Ray, S.K., Chakrabarti, M., Morre, J.D., Coley, H.M., Honoki, K., Fujii, H., Georgakilas, A.G., Amedei, A., Niccolai, E., Amin, A., Ashraf, S.S., Helferich, W.G., Yang, X., Boosani, C.S., Guha, G., Bhakta, D., Ciriolo, M.R., Aquilano, K., Chen, S., Mohammed, S.I., Keith, W.N., Bilsland, A., Halicka, D., Nowsheen, S., Azmi, A.S., 2015. Broad targeting of resistance to apoptosis in cancer. Semin. Cancer Biol. 35 (Suppl. l), S78–S103.

Pak, P.J., Kang, B.H., Park, S.H., Sung, J.H., Joo, Y.H., Jung, S.H., Chung, N., 2016. Antitumor effects of herbal mixture extract in the pancreatic adenocarcinoma cell line PANC1. Oncol. Rep. 36 (5), 2875–2883.

Pinto, B., Henriques, A.C., Silva, P.M.A., Bousbaa, H., 2020. Three-dimensional spheroids as in vitro preclinical models for cancer research. Pharmaceutics 12 (12).

Porta, C., Paglino, C., Mosca, A., 2014. Targeting PI3K/Akt/mTOR signaling in cancer. Front. Oncol. 4, 64.

Qu, Y., Safonova, O., De Luca, V., 2019. Completion of the canonical pathway for assembly of anticancer drugs vincristine/vinblastine in Catharanthus roseus. Plant J. 97 (2), 257–266.

Reczek, C.R., Chandel, N.S., 2017. The two faces of reactive oxygen species in cancer. Annu. Rev. Cell Biol. 1 (1), 79–98.

Salaroglio, I.C., Mungo, E., Gazzano, E., Kopecka, J., Riganti, C., 2019. ERK is a pivotal player of chemo-immune-resistance in cancer. Int. J. Mol. Sci. 20 (10).

Sederholm, C., Hillerdal, G., Lamberg, K., Kolbeck, K., Dufmats, M., Westberg, R., Gawande, S.R., 2005. Phase III trial of gemcitabine plus carboplatin versus single-agent gemcitabine in the treatment of locally advanced or metastatic non-small-cell lung cancer: the Swedish Lung Cancer Study Group. J. Clin. Oncol. 23 (33), 8380–8388.

Sengupta, P., Raman, S., Chowdhury, R., Lohitesh, K., Saini, H., Mukherjee, S., Paul, A., 2017. Evaluation of apoptosis and autophagy inducing potential of Berberis aristata, Azadirachta indica, and their synergistic combinations in parental and resistant human osteosarcoma cells. Front. Oncol. 7, 296.

Shi, G.X., Wang, T.M., Wu, S.B., Wang, Y.X., Shao, J., Zhou, M.Q., Wang, C.Z., 2017. [Activity of essential oil extracted from Artemisia argyi in inducing apoptosis of Candida albicans]. Zhongguo Zhongyao Zazhi 42 (18), 3572–3577.

Shibue, T., Weinberg, R.A., 2017. EMT, CSCs, and drug resistance: the mechanistic link and clinical implications. Nat. Rev. Clin. Oncol. 14 (10), 611–629.

Siegel, R.L., Miller, K.D., Jemal, A., 2020. Cancer statistics, 2020. Ca - Cancer J. Clin. 70 (1), 7–30.

Song, X., Wen, X., He, J., Zhao, H., Li, S., Wang, M., 2019. Phytochemical components and biological activities of Artemisia argyi. J. Funct.Foods 52, 648–662.

Tseng, C.P., Huang, Y.L., Chang, Y.W., Liao, H.R., Chen, Y.L., Hsieh, P.W., 2020. Polysaccharide-containing fraction from Artemisia argyi inhibits tumor cell-induced platelet aggregation by blocking interaction of podoplanin with C-type lectin-like receptor 2. J. Food Drug Anal. 28 (1), 115–123.

Venditto, V.J., Simanek, E.E., 2010. Cancer therapies utilizing the camptothecins: a review of the in vivo literature. Mol. Pharm. 7 (2), 307–349.
Wang, X., Welsh, N., 2014. Bcl-2 maintains the mitochondrial membrane potential, but fails to affect production of reactive oxygen species and endoplasmic reticulum stress, in sodium palmitate-induced beta-cell death. Ups. J. Med. Sci. 119 (4), 306–315.
Wang, Y., Li, J., Chen, Q., Zhou, J., Xu, J., Zhao, T., Huang, B., Miao, Y., Liu, D., 2022. The role of antifungal activity of ethyl acetate extract from Artemisia argyi on Verticillium dahliae. J. Appl. Microbiol. 132 (2), 1343–1356.
Weinberg, S.E., Chandel, N.S., 2015. Targeting mitochondria metabolism for cancer therapy. Nat. Chem. Biol. 11 (1), 9–15.
Woo, Y., Oh, J., Kim, J.S., 2017. Suppression of Nrf2 activity by chestnut leaf extract increases chemosensitivity of breast cancer stem cells to paclitaxel. Nutrients 9 (7).
Wu, X., Zhuang, J., Bai, Z., Guo, D., 2020. In vivo antidiabetic activity of qwueous extract of Artemisia argyi (Chinese mugwort) in alloxan-induced diabetic rats. Trop. J. Pharmaceut. Res. 19 (7), 1487–1493.
Xiao, J.Q., Liu, W.Y., Sun, H.P., Li, W., Koike, K., Kikuchi, T., Yamada, T., Li, D., Feng, F., Zhang, J., 2019. Bioactivity-based analysis and chemical characterization of hypoglycemic and antioxidant components from Artemisia argyi. Bioorg. Chem. 92, 103268.
Xue, G.M., Han, C., Chen, C., Li, L.N., Wang, X.B., Yang, M.H., Gu, Y.C., Luo, J.G., Kong, L.Y., 2017. Artemisians A-D, diseco-guaianolide involved heterodimeric [4 + 2] adducts from artemisia argyi. Org. Lett. 19 (19), 5410–5413.
Yoshikawa, M., Shimada, H., Matsuda, H., Yamahara, J., Murakami, N., 1996. Bioactive constituents of Chinese natural medicines. I. New sesquiterpene ketones with vasorelaxant effect from Chinese moxa, the processed leaves of Artemisia argyi Levl. et Vant.: moxartenone and moxartenolide. Chem. Pharm. Bull. (Tokyo) 44 (9), 1656–1662.
Yun, C., Jung, Y., Chun, W., Yang, B., Ryu, J., Lim, C., Kim, J.H., Kim, H., Cho, S.I., 2016. Anti-inflammatory effects of artemisia leaf extract in mice with contact dermatitis in vitro and in vivo. Mediat. Inflamm. 2016, 8027537.
Zatloukal, P., Petruzelka, L., 2002. Gemcitabine/carboplatin in advanced non-small cell lung cancer. Lung Cancer 38 (Suppl. 2), S33–S36.
Zhang, L.-B., Lv, J.-L., Chen, H.-L., Yan, X.-Q., Duan, J.-A., 2013. Chemical constituents from Artemisia argyi and their chemotaxonomic significance. Biochem. Systemat. Ecol. 50, 455–458.
Zhang, X.W., Wang, S., Tu, P.F., Zeng, K.W., 2018. Sesquiterpene lactone from Artemisia argyi induces gastric carcinoma cell apoptosis via activating NADPH oxidase/reactive oxygen species/mitochondrial pathway. Eur. J. Pharmacol. 837, 164–170.
Zhu, L., Chen, L., 2019. Progress in research on paclitaxel and tumor immunotherapy. Cell. Mol. Biol. Lett. 24, 40.
Zimmermann-Klemd, A.M., Reinhardt, J.K., Morath, A., Schamel, W.W., Steinberger, P., Leitner, J., Huber, R., Hamburger, M., Grundemann, C., 2020. Immunosuppressive activity of artemisia argyi extract and isolated compounds. Front. Pharmacol. 11, 402.